



**HAL**  
open science

## A Carboniferous Apex for the late Paleozoic Icehouse

N. Griffis, R. Mundil, I. Montanez, D. Le Heron, Pierre Dietrich, R. Iannuzzi

► **To cite this version:**

N. Griffis, R. Mundil, I. Montanez, D. Le Heron, Pierre Dietrich, et al.. A Carboniferous Apex for the late Paleozoic Icehouse. S. G. Lucas, W. A. DiMichele, S. Opluštil, X. Wang (Eds.). Ice Ages, Climate Dynamics and Biotic Events: the Late Pennsylvanian World, 535 (1), Geological Society, London, 2023, Geological Society, London, Special Publications, 10.1144/SP535-2022-256 . insu-03976892

**HAL Id: insu-03976892**

**<https://insu.hal.science/insu-03976892>**

Submitted on 7 Feb 2023

**HAL** is a multi-disciplinary open access archive for the deposit and dissemination of scientific research documents, whether they are published or not. The documents may come from teaching and research institutions in France or abroad, or from public or private research centers.

L'archive ouverte pluridisciplinaire **HAL**, est destinée au dépôt et à la diffusion de documents scientifiques de niveau recherche, publiés ou non, émanant des établissements d'enseignement et de recherche français ou étrangers, des laboratoires publics ou privés.

Accepted Manuscript

## *Geological Society, London, Special Publications*

### A Carboniferous Apex for the late Paleozoic Icehouse

N. Griffis, R. Mundil, I. Montanez, D. Le Heron, P. Dietrich & R. Iannuzzi

DOI: <https://doi.org/10.1144/SP535-2022-256>

To access the most recent version of this article, please click the DOI URL in the line above. When citing this article please include the above DOI.

Received 19 August 2022

Revised 3 January 2023

Accepted 3 January 2023

© 2023 The Author(s). Published by The Geological Society of London. All rights reserved. For permissions: <http://www.geolsoc.org.uk/permissions>. Publishing disclaimer: [www.geolsoc.org.uk/pub\\_ethics](http://www.geolsoc.org.uk/pub_ethics)

#### **Manuscript version: Accepted Manuscript**

This is a PDF of an unedited manuscript that has been accepted for publication. The manuscript will undergo copyediting, typesetting and correction before it is published in its final form. Please note that during the production process errors may be discovered which could affect the content, and all legal disclaimers that apply to the book series pertain.

Although reasonable efforts have been made to obtain all necessary permissions from third parties to include their copyrighted content within this article, their full citation and copyright line may not be present in this Accepted Manuscript version. Before using any content from this article, please refer to the Version of Record once published for full citation and copyright details, as permissions may be required.

## **A Carboniferous Apex for the late Paleozoic Icehouse**

N. Griffis<sup>1\*</sup>, R. Mundil<sup>2</sup>, I. Montañez<sup>3</sup>, D. Le Heron<sup>4</sup>, P. Dietrich<sup>5</sup> and R. Iannuzzi<sup>6</sup>

<sup>1</sup> *U. S. Geological Survey, Geology Geochemistry and Geophysics Science Center, Lakewood, CO 80225, ngriffis@usgs.gov \*Corresponding author.*

<sup>2</sup> *Berkeley Geochronology Center, 2455 Ridge Rd, Berkeley, CA, 94709*

<sup>3</sup> *University of California, Davis, One Shield Ave, Davis, CA, 95618*

<sup>4</sup> *Department of Geodynamics and Sedimentology, University of Vienna, Althanstrasse 14, A-1090 Vienna, Austria*

<sup>5</sup> *Géosciences-Rennes, UMR6118, Université de Rennes 1, 35042 Rennes Cedex, France*

<sup>6</sup> *Departamento de Paleontologia e Estratigrafia, Universidade Federal Rio Grande do Sul, Porto Alegre, Rio Grande do Sul 90040-060, Brazil*

### **Abstract**

Icehouse climate systems occur across an abbreviated portion of Earth history, comprising ~25% of the Phanerozoic record. The Late Paleozoic Ice Age (LPIA) was the most extreme and longest lasting glaciation of the Phanerozoic and is characterized by periods of acute continental scale glaciation, separated by periods of ice minima or ice-free conditions on the order of  $<10^6$  years. The late Paleozoic glaciogenic record of the Paraná and Kalahari basins of southern Gondwana form one of the largest, best preserved, and well calibrated records of this glaciation. In the Carboniferous, the eastern and southern margins of the Paraná Basin and the Kalahari Basin were characterized by subglacial conditions, with evidence for continental and upland glaciers. In the latest Carboniferous, these basins transitioned from

subglacial reservoirs to ice-free conditions evidenced by the widespread deposition of marine deposits juxtaposed on subglacial bedforms. High-precision U-Pb zircon CA-TIMS geochronologic constraints from volcanic ash deposits in the deglacial marine black shales of the Kalahari Basin and from fluvial and coal successions, which overlie marine deposits in the Paraná, indicate subglacial evidence in these regions is constrained to the Carboniferous. The loss of ice in these regions is congruent with a late Carboniferous peak in  $p\text{CO}_2$  and widespread marine anoxia in the late Carboniferous. The permeant retreat of glaciers in basinal settings, despite an early Permian  $p\text{CO}_2$  nadir, highlight the influence of short-term perturbations on the longer-term  $\text{CO}_2$  record and suggests an ice-threshold had been crossed in the latest Carboniferous. A definitive driver for greenhouse gases in the LPIA, such as abundant and sustained volcanic activity or an increased biologic pump driven by ocean fertilization, is unresolved for this period. Lastly, the proposed Carboniferous apex for the high-latitude LPIA record is incongruent with observations from the low-latitude tropics where an early Permian peak is proposed.

## Introduction

The Late Paleozoic Ice Age (LPIA) was the most severe and longest lasting glaciation of the Phanerozoic and the only example of an icehouse-greenhouse turnover in a world colonized by complex terrestrial life (Gastaldo, 1996; Montañez and Poulsen, 2013). Interpretation of the nature, scale and dynamics of the late Paleozoic ice record has evolved from a single massive ice sheet centered over polar Gondwana, which lasted for the extent of the ~60 Myr icehouse, to a more dynamic record, one characterized by multiple continental and alpine ice centers with phases of intense glaciation, separated by shorter intervals of diminished ice (Fielding et al., 2008; Isbell et al., 2008; Montañez, 2022). The LPIA glacial record is interpreted as diachronous, with deglaciation occurring first in alpine regions of southwest Gondwana by late Viséan, whereas large ice masses lasted at least into the late early Permian in polar Gondwana (Gulbranson et al., 2011; Isbell et al., 2012; Griffis et al., 2019; Griffis et al., 2021). A diachronous ice-record highlights the importance of long term ( $10^6$  to  $10^8$  years) tectonic constraints (i.e., topography and latitude) on Gondwanan ice distribution (Isbell et al., 2012; Griffis et al., 2019). An exportable chronostratigraphic framework based on high-resolution U-Pb zircon geochronology, developed over recent years for southern Gondwana, provides radioisotopic age constraints on the ice record and reveals the presence of isochronous deglaciation events which can be correlated at the  $<10^6$ -year timescale, and are ~1-2 Myr in duration. The presence of widespread, short-lived deglaciation events suggests a shorter duration, climate-forcing driver of late Paleozoic climatic amelioration (Griffis et al., 2019).

At least three major isochronous deglaciation events are documented across southern and southwestern Gondwana, occurring at ~300–299 Ma, 296 Ma and 282 Ma (Griffis et al., 2019). Deglaciation events correspond with increased  $p\text{CO}_2$ , highlighting the influence of climatic forcing on the Gondwanan glacial record (Griffis et al., 2019; Griffis et al., 2021).

The latest Carboniferous event (300–299 Ma) was one of the most acute and associated with unrecoverable ice across large regions of Gondwana and suggests a late Carboniferous apex of the LPIA (Chen et al., 2016; Griffis et al., 2019; Griffis et al., 2021; Chen et al., 2022).

The late Carboniferous was a period of pronounced climatic change associated with periods of near doubling of  $p\text{CO}_2$  from middle-Carboniferous lows, the repeated turnover of plant communities across the Euramerican tropics, ocean anoxia accompanied by widespread deposition of black shales in marine depositional basins, and the loss of glaciogenic deposits across much of southern Gondwana (Cleal et al., 2005; Moñtanez and Poulsen 2013; Moñtanez et al., 2016; Richey et al., 2020; Chen et al., 2022). Southern Gondwana depositional basins record a rich archive of the response to late Paleozoic climatic forcing, with many basins transitioning from ice proximal and sub-glacial to ice-free or ice distal reservoirs by the late Carboniferous. In particular, the mid- to high-latitude Paraná and Kalahari basins of Brazil and Namibia, respectively, hosts arguably the world's highest fidelity record of this transition given the abundance of core and outcrop data across these passive intracratonic basins, the well-preserved nature of glacial record, and the large area over which glaciogenic deposits can be traced. Sedimentologic studies and detrital zircon geochronology have documented one of the richest Phanerozoic archives of the dynamic nature of late Paleozoic glaciation in this region, documenting a glaciogenic record characterized by multiple advance-retreat cycles before transitioning into post glacial marine or littoral depositional systems (Vesely et al., 2015; Mottin et al., 2018; Vesely et al., 2018; Fedorchuk et al., 2019a; Fedorchuk 2019b; Griffis et al., 2019b; Zieger et al., 2019 Le Heron et al., 2021; Dietrich et al., 2021). Furthermore, high-resolution U-Pb zircon chemical abrasion - thermal ionizing mass spectrometry (CA-TIMS) calibrated ages for these successions allows for the establishment of a multi-basin stratigraphic framework across this

region, which can be used to investigate the nature of the mid to late Carboniferous glaciogenic system.

In this contribution, we briefly review the late Carboniferous and earliest Permian sedimentologic and stratigraphic histories of the Paraná and Kalahari basins with a particular focus on the nature of the glaciation across this region and the ensuing climatic transition. We show that the Carboniferous was an apex of ice extent for the late Paleozoic icehouse across much of southern Gondwana, which was succeeded by an abrupt late Carboniferous warming. We explore some of the possible drivers for ice loss, which are still unresolved. Furthermore, our observations of unrecoverable high latitude ice in the latest Carboniferous presents a paradox, where high latitude ice sheets are collapsing, at a time when high elevation areas in the low latitudes are proposed to experience glacial conditions (Sorgehan et al., 2008; Sorgehan et al., 2014; Sorgehan et al., 2019; Pfiefer et al., 2021). Additionally, we briefly review the glaciogenic record from Gondwana and the temporal constraints for these deposits.

### **Nature and Temporal Constraints of Southwest Gondwana Late Paleozoic Glacial Record**

Late Paleozoic glaciogenic rocks are found on all continents which comprise the supercontinent of Gondwana (Isbell et al., 2003; Milani and De Witt, 2008; Linol et al., 2016; Lopez-Gamundi et al., 2021; Moñtanez et al., 2022). The stratigraphic histories of the intracratonic Paraná and Kalahari basins form one of the highest fidelity records of the LPIA and the ultimate turnover to greenhouse climate conditions by the late early Permian. The Paraná and Kalahari basins cover an area of  $\sim 3 \times 10^6$  km<sup>2</sup>, spanning the mid- to high latitudes of southwest and southern Gondwana ( $\sim 50^\circ$  S Paraná;  $65^\circ$  S Kalahari; Fig. 1; Griffis et al., 2021). Importantly, these intracratonic basins experienced minimal tectonic influence, with

flat lying glaciogenic rocks traced laterally over large areas in outcrop or through core and are often capped by Mesozoic flood basalts, preserving one of the best sedimentologic archives of the LPIA (Milani and De Witt, 2008; Dietrich et al., 2021). In outcrop, the stratigraphic arrangement of facies across this region is largely similar, with all basins typically hosting a major subglacial unconformity along the basin margins, occurring between Precambrian-Cambrian or Devonian basement, and which is typically overlain by either glacial marine, glacial lacustrine or continental glaciogenic deposits (Gonzales and Eyles, 1995). The glaciogenic system often records multiple ice advance-retreat cycles, which manifest as subglacial or ice proximal facies that are overlain by deeper water depositional facies and eventually capped by fluvial/deltaic successions (Holz et al., 2010; Visser et al., 1983; Visser, 1997; Fallgatter and Paim 2019; Griffis et al., 2019; Griffis et al., 2021). Here, we briefly discuss the nature and dynamics of the southern Gondwana glaciogenic record, with a particular focus on an acute late Carboniferous deglaciation and the immediate post glacial successions of southern Brazil and Namibia. The Paraná and Kalahari basins have been the targets for multiple geochronologic studies, focused on refining the age control for the late Paleozoic succession and Gondwanan glaciations (c.f. Bangert et al., 2000; Stolhofen et al., 2008; Cagliari et al., 2016). An extensive review of the previous studies can be found in Griffis et al., 2018; Griffis et al., 2019; Griffis et al., 2021. In this contribution we concentrate on areas where U-Pb zircon CA-TIMS ages are reported, which is considered one of the most accurate and precise geochronologic methods and enables the establishment of regional stratigraphic framework to test the synchronicity and timing of ice loss across these basins.

### *Paraná Basin*

The Paraná Basin is one of the largest depocenters of late Paleozoic rocks in South America (Fig. 1), where glaciogenic deposits cover an area of  $1 \times 10^6$  km<sup>2</sup> and reaching up to



1.3 km in thickness in subsurface cores (Eyles et al., 1993; Rocha-Campos et al., 2008). The glaciogenic rocks are constrained to the Itararé Group, which records anywhere from one to five glacial-interglacial cycles across the Lagoa Azul through Taciba Formations (Vesely et al., 2015; Griffis et al., 2019b). In this contribution we focus solely on the records from Rio Grande do Sul and Santa Catarina states, where the glaciogenic facies attain a thickness from 10's (Rio Grande do Sul State, southern Paraná Basin) to 100's of meters (Santa Catarina State, southeastern Paraná Basin; Fig. 2). In these southern regions the glaciogenic record is highly dynamic, recording multiple ice advance-retreat cycles, interpreted to represent glacial continental and glacial marine facies, with the thickest and most continuous deposits occurring across the southeastern Paraná Basin within Santa Catarina State. Thick fluvial, estuarine and coal deposits cap the glaciogenic systems and host U-Pb zircon dated volcanic ash horizons, which provide age constraints for the final demise of ice in this region. Here we briefly review the glaciogenic and immediate post glacial record from Rio Grande do Sul and Santa Catarina states and the established chronostratigraphic framework for the region.

Subglacial erosional features which include scoured paleovalleys, roche moutonnée, striated pavements and larger streamlined bedrock features record the initial advance of glaciers across the southern Paraná Basin (Fig. 2 & 3A; Gesicki et al., 2002; Rocha-Campos et al., 2008; Assine et al., 2019). In Rio Grande do Sul State, push moraine complexes which record multiple advance-retreat cycles, striated pavements and soft sediment deformed glacial plow structures indicate the presence of dynamic grounded glaciers across southern Brazil (Fig. 2 & 3A; Tomazelli and Junior 1996; Fedorchuk et al., 2019b). In Uruguay, ~100 km to the south of Rio Grande do Sul State, asymmetrical stream lined landforms, interpreted as whale backs, which formed by the erosion of an overriding glacier, confirms the presence of grounded ice in this region (Assine et al., 2019). In Santa Catarina State (southeast Paraná Basin), paleovalleys up to 500 m wide and 40 m deep, were carved into Precambrian

basement along the eastern margin of the basin, recording the initial ice advance. Linear striations, as well as gouged and polished surfaces, which are found within and along the margins of the paleovalleys, attest to subglacial erosion. The paleovalley infill records multiple ice advance-retreat cycles, composed of marine black shales, rhythmites, mass transport and dropstone poor diamictites, indicating a dynamic glaciation (Fig. 2 & 3C; Fallgatter and Paim, 2019). Paleoflow indicators across the south and southeast margin of the Paraná Basin suggests an overall north to northwest flow of ice into the basin, with ice emanating from at least two distinct African ice centers (Fig. 1; Gesicki et al., 2002; Rosa et al., 2016; Assine et al., 2019; Griffis et al., 2019b; Fedorchuk et al., 2021; Griffis et al., 2021). Detrital zircon geochronology from across the south and southeast margin of the Paraná Basin confirms an African ice source (Griffis et al., 2019b; Fedorchuk et al., 2021). The anatomy of the deglaciation successions across the Paraná Basin generally involves the juxtaposition of “deeper water” facies, directly on top of the subglacial surfaces and include finely laminated rhythmites, organic-rich mudstones as well as glacially influenced mass transport deposits (Fig. 2 and 3C; Fedorchuk et al., 2019; Valdez Buso et al., 2019). Generally, one to two deglaciation successions are found in southern Paraná Basin in Brazil and Uruguay, whereas at least three and as many as five are found along the southeast margin of the Paraná Basin (Assine et al., 2019; Vesley et al., 2015; Mottin et al., 2018; Fedorchuk et al., 2019; Fallgatter and Paim, 2019). The latest glaciogenic deposits, referred to as the Rio Do Sul or Taciba formations are capped by fluvial sandstones and coals of the lower part of the Rio Bonito Formation (Guatá Group), which often host volcanic ash layers containing zircon that are used to refine interbasinal correlations and calibrate the glaciogenic record (Fig. 2 and Fig 3G; Holz et al., 2010; Cagliari et al., 2016; Griffis et al., 2018). The Rio Bonito Formation of the Guatá Group is characterized by a highly dynamic base-level record, which has been correlated to the waxing and waning of higher-latitude glaciation (Griffis et

al., 2019a). The lower part of the Rio Bonito Formation is characterized by fluvial sandstones, estuarine and coal facies, which sit directly on deep water marine deposits, or are incised into local basement (Holz et al., 2010). The Itararé Group- Rio Bonito Formation contact is recognized as region sequence boundary that can be traced across the Paraná Basin and which formed as a result of a forced regression (Holz et al., 2008; Griffis et al., 2019).

The lower part of the Rio Bonito Formation, which directly overlies the glaciogenic facies of the Itararé Group across the Paraná Basin, is rich in volcanic ash deposits. Five of the ash deposits have been dated using high-resolution U-Pb zircon CA-TIMS methods and provide age constraints for the demise of glaciation across this region (Griffis et al., 2018; Fig. 2). Three of the U-Pb zircon CA-TIMS ages are from tonsteins (HNC, CT1, and CT3), which are hosted within the coal deposits surrounding the village of Candiota in Rio Grande do Sul State. One age comes from an isolated outcrop (QUT), which is in central Rio Grande do Sul, 150 km northeast of Candiota (Fig 2 & Fig 3G). The U-Pb ages from the lower part of the Rio Bonito Formation range from  $298.23 \pm 0.31$  Ma to  $296.97 +0.45/-0.72$  Ma (Griffis et al., 2018). An additional U-Pb zircon age of  $297.4 + 1.13/- 1.19$  Ma was reported from an ash (ANT1) sampled in fluvial deltaic facies located 60 m above the Guatá-Itararé Group contact in the lower part of the Rio Bonito Formation from the Anitápolis core in Santa Catarina State (Figs 2 and 3H; Griffis et al., 2019a). Importantly, the Anitápolis core contains the same stratigraphy and is located within the vicinity of the paleovalley successions described by Fallgatter and Paim (2019), confirming a Carboniferous age for the glacial facies in this region (Griffis et al., 2018; Griffis et al., 2019; Griffis et al., 2021).

### *Kalahari Basin*

The Kalahari Basin covers an area greater than  $2.5 \times 10^6$  km<sup>2</sup>, extending across Namibia, Botswana as well as parts of Zimbabwe, Zambia, South Africa, and Angola (Fig 1; Visser et

al., 1983; Visser et al., 1997; Catuneanu et al., 2005). Glaciogenic deposits in southern Africa are constrained to the Dwyka Group (Fig. 2), which occurs in outcrop along the margins of the Kalahari Basin and found in core across much of this region (Frakes and Crowell, 1970; Visser, 1983; Cairncross, 2001; Linol et al., 2016; Dietrich et al., 2019). The Dwyka Group attains a maximum thickness of 800 m in the Karoo Basin of South Africa, where the Group is defined, and reaches a maximum thickness of ~200 m in outcrop across southern Namibia (Fig. 2; Visser et al., 1997; Stolhoffen et al., 2008). The Dwyka Group records a highly dynamic glaciogenic record, which is divided into four ice advance-retreat cycles, referred to as deglaciation sequences (DS), which are defined in South Africa by a lower subglacial or ice proximal unit that is overlain by deeper water ice-distal or ice-free deposits (Visser et al., 1997; Isbell et al., 2008). Marine mudstones of the Ecca Group directly overlie the Dwyka Group deposits and mark the demise of ice in this region (Visser, 1997). Deglaciation sequences have been correlated across southern Africa, through high-resolution U-Pb zircon CA-TIMS analysis, challenging some of the previous correlations, as the Kalahari Basin was ice free 12 million years prior to the Karoo Basin (Griffis et al., 2021). Here we briefly review some of the subglacial and the immediate postglacial record in the Kalahari Basin as well as the current temporal constraints on the deposits.

Namibia hosts one of the highest fidelity records of the late Paleozoic glaciation, preserving ancient fjord networks, a complex basal unconformity that extends for 100's of kms in outcrop and large linear erosional features including drumlins, which attest to the subglacial history of this region (Figs 2 and 3B; Martin 1981; Dietrich et al., 2019; Andrews et al., 2019; le Heron et al., 2021). During the acme of the LPIA a large, at least 1.7 km thick, ice sheet covered northern Namibia (Dietrich et al., 2021). Deeply incised paleovalleys, up to 1 km in depth and 5 km in width, can be traced for 10-100's of km and are interpreted to have been carved by an icesheet which propagated across northern Namibia and into the Paraná

Basin (Fallgatter and Paim, 2019; Rosa et al., 2019; Dietrich et al., 2021). Polished and striated surfaces as well as diamictite are found above and outside the valley walls indicating that these regions were overtopped by ice during the acme of the glaciation (Martin 1981; Dietrich et al., 2021). Additional scoured and striated surfaces are preserved along the floor and walls of the valleys, with multiple stepped levels of marginal moraine interpreted as recording ice advance-retreat cycles (Dietrich et al., 2021). Ultimately, these valleys were filled with marine rocks and given the scale and well-preserved nature of the deposits are regarded as one of the world's best-preserved examples of a pre-Cenozoic fjord network (Dietrich et al., 2021; Le Heron et al., 2022). In southern Namibia, equally impressive outcrops within the Aranos and Karasburg subbasins of the greater Kalahari, record a complex system of fluvial incision, subglacial erosion, and ice proximal deposits, which overlie unconformably Precambrian-Cambrian basement attesting to the growth and progradation of ice across this region (Stollhofen et al., 2008; Le Heron et al., 2021). Boulder beds striated and polished surfaces, and subglacial shearing of unconsolidated sediments are documented across these regions and confirm subglacial and proglacial conditions (Figs. 2, 3B and 3E; Visser, 1983; Le Heron et al., 2021). The subglacial deposits across southern Namibia are overlain by a distinct 20-50 m thick black shale facies, referred to as the Ganigobis Shale Member (Aranos subbasin) or Zwartbas shale (Karasburg subbasin), which represent a major marine transgression, which formed as a result of abrupt ice loss during DSII (Figs 2 and 3D; Werner et al., 2006; Stollhofen et al., 2008). These black shales mark the demise of subglacial evidence across this region of Gondwana (Visser et al., 1997; Griffis et al., 2021). In addition, the Ganigobis Shale Member incorporates columnar limestone deposits, which are interpreted to have formed around methane seeps (Himmler et al., 2008; Birgel et al., 2008). At least one glaciogenic horizon occurs above the Ganigobis Shale Member and the correlative shales near Zwartbas (Fig 2). The final demise of ice in Namibia

is associated with the deposition of mudstones from the Ecca Group, which overlies the uppermost glaciogenic rocks.

The Ganigobis Shale Member and the black shales near Zwartbas directly overlie the subglacial facies of the lower part of the Dwyka Group in Namibia and contain volcanic ash layers, which have been dated radio isotopically and provide age control for the disappearance of grounded ice in this region (Werner, 2006; Stolhoffen et al., 2008). High-resolution U-Pb CA-TIMS analyses from three volcanic ash units indicate that the deposition of the black shales was synchronous and constrained to the latest Carboniferous. Two volcanic ashes sampled 5 and 7 m above the subglacial facies of the lower part of the Dwyka Group in the shales near Zwartbas within the Karasburg subbasin yield ages between  $300.45 \pm 0.37$  and  $299.41 \pm 0.24$  Ma, respectively (Fig. 2). In the Aranós subbasin, a similar age of  $299.31 \pm 0.35$  Ma was reported from an ash unit sampled in the Ganigobis Shale Member, 5 m above the contact with the underlying glaciogenic facies (Figs. 2 and 3F). The reported late Carboniferous ages for the black shales indicate an abrupt latest Carboniferous warming responsible for the demise of subglacial ice in this region. Glacially influenced deposits, occur above these shales, in the upper part of the Dwyka Group including debris flow diamict and dropstones, though no subglacial evidence is found in this region. The final demise of ice in Namibia is constrained by an ash bed (OG-09) dated at  $295.84 \pm 0.47$  Ma, 7 meters above the Dwyka Group-Prince Albert Formation contact, in the lower part of the Ecca Group of the Karasburg basin (Fig. 2; Griffis et al., 2021).

The late Paleozoic sedimentary record of the Paraná and Kalahari basins records the transition from subglacial reservoirs to ice-free conditions across southwest Gondwana by the latest Carboniferous. During peak glaciation in the Carboniferous, glaciers occupied the mid- to high-latitude continental and upland regions with evidence for dynamic wet based glaciers occurring along basin margins or near subglacial ice streams (Visser 1983; Rosa et al., 2019;

Fedorchuk 2019; Le Heron et al., 2022). Glaciers carved valleys in the upland regions and ice sheets emanated across southern Africa and into South America (Isbell et al., 2012; Fallgater and Paim 2019; Assine et al., 2019; Rosa et al., 2019; Fedorchuk et al., 2021; Dietrich et al., 2022; Le Heron et al., 2022). Detrital zircon geochronology from glaciogenic deposits confirm these findings, with zircons with African provenance recovered from Paraná Basin glaciogenic deposits (Griffis et al., 2019b; Fedorchuk 2021; Griffis et al., 2021). The latest Carboniferous was associated with an abrupt change in the style and distribution of Gondwana glaciers, where once subglacial basins transitioned to nonglacial marine conditions in the Kalahari and Paraná regions. In the Paraná Basin, the Rio Do Sul and Taciba formations contain the last glacially influenced deposits in the region and are temporally correlative with the Ganigobis Shale Member of Namibia (Fig. 2). The demise of glaciers within these basins is coincident with a near doubling of  $p\text{CO}_2$ , from middle Carboniferous lows to late Carboniferous, where values are 2x present atmospheric level (PAL), though forcing mechanisms related to the abrupt release of  $p\text{CO}_2$  are unresolved (Richey et al., 2020; Moñtanez, 2022).

### **Abrupt late Carboniferous Warming**

On the  $>10^6$ -year timescales, icehouse climate systems are largely driven by changes in the sinks and sources of greenhouse gases. Sinks include silicate weathering in the tropics, deliverability of alkalinity to ocean basins, and the burial of organic matter and are counter-balanced by the release of greenhouse gases through processes such as volcanism (Nelson et al., 2016; McKenzie et al., 2016; MacDonald et al., 2019). The late Carboniferous and early Permian is characterized by a highly variable  $p\text{CO}_2$  record, with a late Carboniferous peak (~304 Ma; 600 ppmv) followed by a nadir in the earliest Permian (~298 Ma; 200 ppmv; Richey et al., 2020). The latest Carboniferous warming is coincident with ocean anoxia and the demise of Gondwanan glaciers, whereas the nadir at the earliest Permian is associated

with the return of glaciogenic conditions in regions surrounding the Kalahari and Karoo basins, and low stand sedimentation in the Paraná Basin (Griffis et al., 2019; Chen et al., 2022). Punctuated warming events in the late Carboniferous overprint the longer-term trend of decreasing  $p\text{CO}_2$  through the early Permian indicating a likely short-lived, high-volume release of greenhouse gas which overprints the longer term ( $>10^6$ -year) sink, the latter of which is attributed to weathering (Richey et al., 2020).

Drivers for the abrupt demise of Gondwanan ice are unresolved in the latest Carboniferous. Degassing as a result volcanism is postulated as a main driver for late Paleozoic deglaciation (McKenzie et al., 2016; Yang et al., 2020), whereas other studies invoke volcanism as the main driver of glaciation, caused by negative radiative forcing associated with release of aerosol particles into the stratosphere and an increase ocean biologic pump driven by the fertilization of ocean basins (Soreghan et al., 2019). Constraints on the age and tempo of the proposed drivers are limited to the  $>10^6$ -year timescale, an order of magnitude less precise than the  $p\text{CO}_2$  and ice records from this time period, making it difficult to resolve processes responsible for the demise of glaciation and which ultimately highlights the need for additional geochronologic constraints on glaciogenic deposits and volcanic sources. Lastly, we discuss other possible greenhouse gas sources, such as methane seeps, which may have contributed to the amplification of late Paleozoic deglaciations (Himmler et al., 2008; Haig et al., 2022).

The synchronous demise of glaciers in latest Carboniferous at  $\sim 300$  Ma in the Kalahari and Paraná basins, requires a high-volume short duration release of greenhouse gases. The Skagerrak Centered Large Igneous Province has been proposed as a possible driver (Griffis, 2018; Yang et al., 2020) though current temporal constraints on the Skagerrak Centered Large Igneous Province are coarse, precluding our ability to directly correlate these events. As an example, a current pooled age of  $297 \pm 4$  Ma (weighted mean; Torsvik et al., 2008) for



all volcanic intrusions and eruptions of the Skagerrak Centered Large Igneous Province indicate anywhere between a latest Carboniferous through early Permian record for emplacement. Importantly, a 300–299 Ma age for the top of DSII is congruent with the eruption, as is the return of ice at 298 Ma and DSIII (296 Ma), and therefore deciphering whether the Skagerrak Centered Large Igneous Province was an actual driver of deglaciation or possibly the glaciation is unattainable given that the temporal constraints and quoted uncertainties permit either interpretation.

A volcanic driver of glaciation has also been proposed for the late Paleozoic based on inconsistencies between the  $p\text{CO}_2$  and the ice record, where an earliest Permian peak of glaciogenic deposits is coincident with a peak in global volcanic activity (Soreghan et al., 2019). In this scenario, volcanic aerosols are released into the stratosphere resulting in negative radiative forcing, which was further amplified by fertilizing ocean basins with reactive iron, resulting in an increased biologic pump and carbon sequestration. This hypothesis requires an unprecedented scale and tempo of volcanism given the short residence time of aerosol particles in the stratosphere (cf. Lee and Dee, 2019). Foundational to the volcanic driver hypothesis is a disconnect between  $p\text{CO}_2$  and the ice record, though recent studies have confirmed this connection, where periods of elevated  $p\text{CO}_2$  in the latest Carboniferous are contemporaneous with widespread ice loss (Griffis et al., 2019; Richey et al., 2020; Griffis et al., 2021). The volcanic driver hypothesis also assumes an early Permian apex (298–295 Ma) for the late Paleozoic glaciation, which was established based on the global frequency of glacial diamictites across the LPIA (cf. Soreghan et al., 2019). The frequency of diamictites as a proxy for glacial maximum is limited by the poor temporal constraints on the glaciogenic deposits and the nature, preservation, and representation of the diamict, i.e., ice contact, ice distal deposits, or non-glacial origin (Fedorchuk et al., 2019; Dietrich et al., 2021). The presence of diamictite deposits within a basin does not require

glaciogenic conditions. In fact, detailed field and sedimentologic evidence has shown in many instances that these deposits may have a non-glacial origin or represent mass transport and/or slope failure deposits associated with ice collapse (Dietrich et al., 2019, Fedorchuk et al., 2019b; Rosa et al., 2019). Furthermore, glaciogenic deposits during the late Paleozoic are likely biased towards the demise of the ice record, a result in changes in accommodation space and the nature of glacial processes, and therefore the maximum occurrence of diamictites does not correlate with peak ice (González-Bonorino and Eyles, 1995). The presented histories of the Paraná and Kalahari basins, indicate that all subglacial evidence in these basins is constrained to the Carboniferous, not early Permian, and given the size and latitudinal extents, argues against an early Permian apex for late Paleozoic ice.

In the Kalahari Basin, the widespread occurrence of columnar limestones beds, which formed through microbial activity around hydrocarbon seeps, are associated with the immediate postglacial deposits of the Ganigobis Shale Member (Himmler et al., 2008; Birgel et al., 2008). Similar columnar limestone facies formed around hydrocarbon seeps in black shales in western Australia, directly above glaciogenic deposits in the early Permian (Sakmarian) Holmwood Shale (Haig et al., 2022). In these basins, the limestone columns formed in response to the anaerobic oxidation of methane, evidenced by  $\delta^{13}\text{C}$  values as depleted as -51‰ (Birgel et al., 2008). Importantly, these deposits are also documented in the Cretaceous of the Canadian Arctic, where they are attributed as a driver between cold to warm climate conditions in the latest Albian (Williscroft et al., 2017). While the spatial distribution of methane seeps is not resolved in the late Paleozoic, the immediate occurrence with deglacial black shales merits further investigation, especially given the outsized influence of methane as a greenhouse gas, which is 25x more potent than  $\text{CO}_2$  (Yvon-Durocher et al., 2014).

### **The Carboniferous Apex**

Detailed field studies of glaciogenic reservoirs coupled with recently published high-resolution U-Pb zircon CA-TIMS geochronologic constraints from across the Paraná and Kalahari basins indicate subglacial evidence in these two massive intra-cratonic basins, which span between 45° and 65°S latitude, are restricted to the Carboniferous (Vesely et al., 2018; Fallgater and Paim, 2019; Rosa et al., 2019; Fedorchuk et al., 2019b; Griffis et al., 2019a; Le Heron et al., 2022; Griffis et al., 2021). A Carboniferous apex for the late Paleozoic glaciation in southern Gondwana is incongruent with the accepted early Permian peak. The early Permian apex was established based on the secondary ion mass spectrometry (SIMS) U-Pb zircon calibrated eastern Australian ice record, which indicates maximum ice extent in the early Permian, referred to as (P-1) and stable isotope records from across the low latitudes which show an enrichment in  $\delta^{18}\text{O}$  at this time (Fielding et al., 2008; Koch and Frank 2011). Additional evidence for an early Permian apex of LPIA glaciation include the abrupt juxtaposition of terrestrial successions on marine platforms in the Pangean tropics and the occurrence of widespread silt deposition, which is attributed to upland glaciers (Koch and Frank 2011; Soreghan et al., 2014; Soreghan et al., 2019; Pfieler et al., 2021). In contrast, evidence for a Carboniferous peak is based on the zircon U-Pb CA-TIMS calibrated record from southern Gondwana glaciogenic deposits, the cyclothem records from the mid-continent of the United States and Europe, which are widespread in the Carboniferous and diminish by the early Permian, as well as conodont apatite  $\delta^{18}\text{O}$  oxygen isotope enrichment in the Bashkirian from the Nanjing section of China, and interpreted as the late Paleozoic glacial maximum (Heckel, 1977; Heckel, 2008; Gulbranson et al., 2010; Buggish et al., 2011; Eros et al., 2012; Gulbranson et al., 2010; Chen et al., 2016; Griffis et al., 2018; Griffis et al., 2019).

Reconciling these records and their interpretations is required to gain a better understanding as to the timing and forcing mechanisms responsible for the demise of the LPIA. The Australian glaciogenic record is regarded as one of the best preserved late Paleozoic deposits

and is often used to define the Paleozoic glaciogenic periods (Fielding et al., 2008). The age control used to build this framework, is largely based on in situ analytical techniques on zircon that were not treated for Pb loss and in part compromised by the use of calibration standards which are now known to be heterogeneous (Black et al., 2003). Therefore, new high-precision U-Pb zircon age constraints from Australia are needed to test current stratigraphic assignments. To that extent the U-Pb CA-TIMS calibrated record of the LPIA for southern and western Gondwana is the most precise and accurate temporal framework of late Paleozoic glaciation and is congruent with a Carboniferous peak (Gulbrason et al., 2011; Griffis et al., 2019; Griffis et al., 2021). In addition, the low latitude evidence for glaciation may have more parsimonious non-glacial interpretations. The Unaweep canyon in western Colorado, previously interpreted as an exhumed glacial valley (Soreghan et al., 2008; Soreghan et al., 2014), has been reinterpreted as an exhumed fluvial valley formed through the uplift of the Uncompahgre Plateau in the Cenozoic (Hood et al., 2009; Ronnevik et al., 2017). Widespread silt deposition across the Pangean tropics in the early Permian has also been argued as evidence for upland glaciation in the Central Pangea Mountains (Soreghan et al., 2014; Pfiefer et al., 2021). Radioisotopic age constraints for the silt deposits are lacking in North America, though in the Lodève Basin of France are well constrained to the Sakmarian-Artinskian based on U-Pb zircon maximum depositional ages from zircon recovered in the silts and high precision U-Pb CA-TIMS from volcanoclastic units (Michel et al., 2015; Pfiefer et al., 2021). Importantly, the early Permian was a period of widespread ice loss in polar Gondwana, which was accompanied by the onset of aridification in the tropics as evidenced by the diversification of drought tolerant plants, paleosols enriched in carbonate and smectite clays, and a rise in  $p\text{CO}_2$  (Tabor et al., 2019; Griffis et al., 2019; Richey et al., 2020; Marchetti et al., 2022; Griffis et al., 2023). The lack of any definitive ice contact deposits in

the Pangean tropics, coupled with high latitude ice loss in the early Permian and aridification across this region suggests a likely non glacial origin for the silt.

## Conclusions

The Paraná and Kalahari basins of southern Gondwana preserve one of the most extensive and best calibrated records of the late Paleozoic glaciation. Subglacial landforms, which include fjord networks, striated pavements and roche moutonnée, as well as subglacial or ice contact deposits such as boulder beds and push moraine complexes, formed through erosional processes associated with the expansion of ice sheets and upland glaciers across these regions in the Carboniferous. An acute climatic amelioration occurred in the latest Carboniferous, which is evidenced by the abrupt loss of glaciogenic rocks and the onset of marine conditions in these basins. High-precision U-Pb zircon CA-TIMS geochronologic constraints from volcanoclastic units hosted within the marine shales of Namibia and in fluvial and coal deposits, which overlie the glaciogenic rocks in the Paraná Basin, indicate that these basins were ice-free in the latest Carboniferous (~300 Ma). Importantly, no subglacial evidence is documented in the basins following the late Carboniferous warming, though glaciogenic rocks persist in Namibia through the early Permian (296 Ma). The abrupt and synchronous loss of glaciogenic rocks in southern Gondwana, occurred in tandem with a short-lived rise in  $p\text{CO}_2$ . The unrecoverable loss of subglacial ice in late Carboniferous, despite a return to low  $p\text{CO}_2$  in the earliest Permian, suggests an ice threshold had been crossed in the late Carboniferous and requires a short-term driver of greenhouse gases, such as volcanism. The loss of grounded ice in these basins by the late Carboniferous, suggests the apex of the late Paleozoic icehouse is in the Carboniferous.

Disclaimer: Any use of trade, firm, or product names is for descriptive purposes only and does not imply endorsement by the U.S. Government.

ACCEPTED MANUSCRIPT

## References

- Andrews, G.D., McGrady, A.T., Brown, S.R., Maynard, S.M. 2019. First description of subglacial megalineations from the late paleozoic ice age in Southern Africa. *PLOS ONE*, 14, 1–10, doi:10.1371/journal.pone.0210673
- Assine, M.L., de Santa Ana, H., Veroslavsky, G., Vesely, F.F. 2018. Exhumed subglacial landscape in Uruguay: Erosional landforms, depositional environments, and Paleo-ice flow in the context of the late Paleozoic gondwanan glaciation. *Sedimentary Geology*, 369, 1–12, doi:10.1016/j.sedgeo.2018.03.011
- Bangert, B., Stollhofen, H., Lorenz, V., and Armstrong, R.L. 1999. The geochronology and significance of ash-fall tuffs in the glaciogenic Carboniferous-Permian Dwyka Group of Namibia and South Africa. *Journal of African Earth Sciences*, 29, 33–49, doi:10.1016/S0899-5362(99)00078-0
- Birgel, D., Himmler, T., Freiwald, A., Peckmann, J. 2008. A new constraint on the antiquity of anaerobic oxidation of methane: Late Pennsylvanian seep limestones from southern Namibia. *Geology*, 36, 543–546, doi:10.1130/g24690a.1
- Black, L.P., Kamo, S.L., Williams, I.S., Mundil, R., Davis, D.W., Korsch, R.J., Foudoulis, C. 2003. The application of shrimp to Phanerozoic geochronology; a critical appraisal of four zircon standards. *Chemical Geology*, 200, 171–188, doi:10.1016/s0009-2541(03)00166-9
- Buggisch, W., Wang, X., Alekseev, A.S., Joachimski, M.M. 2011. Carboniferous–Permian carbon isotope stratigraphy of successions from China (yangtze platform), USA (Kansas) and Russia (Moscow basin and Urals). *Palaeogeography, Palaeoclimatology, Palaeoecology*, 301, 18–38, doi:10.1016/j.palaeo.2010.12.015
- Cagliari, J., Philipp, R. P., Buso, V. V., Netto, R. G., Klaus Hillebrand, P., da Cunha Lopes, R., Stipp Basei, M. A., Faccini, U. F. 2016. Age constraints of the glaciation in the Paraná Basin: evidence from new U–Pb dates. *Journal of the Geological Society*, 173, 871–874, doi:10.1144/jgs2015-161
- Cairncross, B. 2001. An overview of the Permian (Karoo) coal deposits of Southern Africa. *Journal of African Earth Sciences* 33, 529–562, doi:10.1016/s0899-5362(01)00088-4  
osa
- Catuneanu, O., Wopfner, H., Eriksson, P.G., Cairncross, B., Rubidge, B.S., Smith, R.M.H., Hancox, P.J. 2005. The Karoo basins of south-Central Africa. *Journal of African Earth Sciences*, 43, 211–253, doi:10.1016/j.jafrearsci.2005.07.007
- Chen, B., Joachimski, M.M., Wang, X.-dong, Shen, S.-zhong, Qi, Y.-ping, Qie, W.-kun. 2016. Ice volume and Paleoclimate History of the late Paleozoic ice age from conodont apatite oxygen isotopes from Naqing (Guizhou, China). *Palaeogeography, Palaeoclimatology, Palaeoecology* 448, 151–161, doi:10.1016/j.palaeo.2016.01.002
- Chen, J., Montañez, I.P., Zhang, S., Isson, T.T., Macarewich, S.I., Planavsky, N.J., Zhang, F., Rauzi, S., Daviau, K., Yao, L., Qi, Y.-ping, Wang, Y., Fan, J.-xuan, Poulsen, C.J.,

- Anbar, A.D., Shen, S.-zhong, Wang, X.-dong. 2022. Marine anoxia linked to abrupt global warming during Earth's penultimate Icehouse. *Proceedings of the National Academy of Sciences* 119, 1–9, doi:10.1073/pnas.2115231119
- Cleal, C.J. and Thomas, B.A. 2005. Palaeozoic tropical rainforests and their effect on global climates: Is the past the key to the present? *Geobiology*, 3, 13–31, doi:10.1111/j.1472-4669.2005.00043.x
- Dietrich, P., Hofmann, A. 2019a. Ice-margin fluctuation sequences and grounding zone wedges: The record of the Late Paleozoic Ice Age in the eastern Karoo Basin (Dwyka Group, South Africa). *The Depositional Record*, 5, 247–271, doi:10.1002/dep2.74
- Dietrich, P., Franchi, F., Setlhabi, L., Prevec, R., Bamford, M. 2019b. The nonglacial diamictite of Toutswe Mogala Hill (lower Karoo supergroup, Central Botswana): Implications on the extent of the Late Paleozoic Ice Age in the Kalahari–Karoo basin. *Journal of Sedimentary Research*, 89, 875–889, doi:10.2110/jsr.2019.48
- Dietrich, P., Griffis, N.P., Le Heron, D.P., Montañez, I.P., Kettler, C., Robin, C., Guillocheau, F. 2021. Fjord network in Namibia: A Snapshot into the dynamics of the late Paleozoic glaciation. *Geology*, 49, 1521–1526, doi:10.1130/g49067.1
- Eros, J.M., Montañez, I.P., Osleger, D.A., Davydov, V.I., Nemyrovska, T.I., Poletaev, V.I. and Zhykalyak, M.V. 2012. Sequence stratigraphy and onlap history of the Donets Basin, Ukraine: Insight into Carboniferous icehouse dynamics. *Palaeogeography, Palaeoclimatology, Palaeoecology*, 313–314, 1–25, doi:10.1016/j.palaeo.2011.08.019
- Eyles, C.H., Eyles, N., Franca, A.B. 1993. Glaciation and tectonics in an active intracratonic basin: The late Palaeozoic Itararé group, Paraná Basin, Brazil. *Sedimentology*, 40, 1–25. doi:10.1111/j.1365-3091.1993.tb01087.
- Fallgatter, C., Paim, P.S.G. 2019. On the origin of the Itararé Group basal nonconformity and its implications for the late Paleozoic glaciation in the Paraná Basin, Brazil. *Palaeogeography, Palaeoclimatology, Palaeoecology* 531, 108225, doi:10.1016/j.palaeo.2017.02.039
- Fedorchuk, N.D., Isbell, J.L., Griffis, N.P., Montañez, I.P., Vesely, F.F., Iannuzzi, R., Mundil, R., Yin, Q.-Z., Pauls, K.N., Rosa, E.L.M. 2019a. Origin of paleovalleys on the Rio Grande do Sul Shield (Brazil): Implications for the extent of late Paleozoic glaciation in west-central Gondwana. *Palaeogeography, Palaeoclimatology, Palaeoecology* 531, 108738, doi:10.1016/j.palaeo.2018.04.013
- Fedorchuk, N.D., Isbell, J.L., Griffis, N.P., Vesely, F.F., Rosa, E.L.M., Montañez, I.P., Mundil, R., Yin, Q.-Z., Iannuzzi, R., Roesler, G., Pauls, K.N. 2019b. Carboniferous glaciotectionized sediments in the southernmost Paraná Basin, Brazil: Ice marginal dynamics and Paleoclimate Indicators. *Sedimentary Geology*, 389, 54–72, doi:10.1016/j.sedgeo.2019.05.006
- Fedorchuk, N.D., Griffis, N.P., Isbell, J.L., Goso, C., Rosa, E.L.M., Montañez, I.P., Yin, Q.-Z., Huyskens, M.H., Sanborn, M.E., Mundil, R., Vesely, F.F., Iannuzzi, R. 2021. Provenance of late Paleozoic glacial/post-glacial deposits in the eastern Chaco-Paraná



Basin, Uruguay and southernmost Paraná Basin, Brazil. *Journal of South American Earth Sciences*, 106, 102989, doi:10.1016/j.jsames.2020.102989

- Fielding, C. R., Frank, T. D., Isbell, J. L., 2008. The late Paleozoic ice age – A review of current understanding and synthesis of global climate patterns. In: Fielding, C. R., Frank, T. D., Isbell, J. L. (Eds.), *Resolving the Late Paleozoic Ice Age in Time and Space*. Geological Society of America Special Paper, 441, 343-354, doi:10.1130/2008.2441(24)
- Frakes, L.A., and Crowell, J.C. 1970. Late Paleozoic glaciation: II. Africa, exclusive of the Karoo Basin. *Geological Society of America Bulletin*, 81, 2261–2286, doi:10.1130/0016-7606(1970)81[2261:LPGIAE]2.0.CO;2
- Gastaldo, R. A., DiMichele, W. A., Pfeifferkorn, H. W. 1996. Out of the icehouse into the greenhouse; a late Paleozoic analog for modern global vegetational change. *Geological Society America Today*, 6, 1–7
- Gesicki, A. L. D., Riccomini, C., Boggiani, P. C. 2002. Ice flow direction during late Paleozoic glaciation in western Paraná Basin, Brazil. *Journal of South American Earth Sciences* 14, 933-939, doi:10.1016/S0895-9811(01)00076-1
- González-Bonorino, G., Eyles, N. 1995. Inverse relation between ice extent and the late Paleozoic glacial record of Gondwana. *Geology*, 23, 1015–1018, doi:10.1130/0091-7613(1995)023<1015:irbiea>2.3.co;2
- Griffis, N. 2018. *From Isotopes to Ice: Refining the late Paleozoic Glaciation in Time and Space*. (Ph.D. Dissertation). University of California, Davis. p. 114.
- Griffis, N. P., Mundil, R., Montañez, I. P., Isbell, J., Fedorchuk, N., Vesely, F., Iannuzzi, R., Yin, Q.-Z. 2018. A new stratigraphic framework built on U-Pb single-zircon TIMS ages and implications for the timing of the penultimate icehouse (Paraná Basin, Brazil). *Geological Society of America Bulletin*, 130, 848–858, doi:10.1130/B31775.1
- Griffis, N.P., Montañez, I.P., Mundil, R., Richey, J., Isbell, J., Fedorchuk, N., Linol, B., Iannuzzi, R., Vesely, F., Mottin, T., da Rosa, E., Keller, B., Yin, Q.-Z. 2019a. Coupled stratigraphic and U-Pb Zircon age constraints on the late Paleozoic icehouse-to-greenhouse turnover in south-central Gondwana. *Geology*, 47, 1146–1150, doi:10.1130/g46740.1
- Griffis, N.P., Montañez, I.P., Fedorchuk, N., Isbell, J., Mundil, R., Vesely, F., Weinshultz, L., Iannuzzi, R., Gulbranson, E., Taboada, A., Pagani, A., Sanborn, M.E., Huyskens, M., Wimpenny, J., Linol, B., Yin, Q.-Z. 2019b. Isotopes to ice: Constraining provenance of glacial deposits and ice centers in west-central Gondwana. *Palaeogeography, Palaeoclimatology, Palaeoecology*, 531, 108745, doi:10.1016/j.palaeo.2018.04.020
- Griffis, N., Montañez, I., Mundil, R., Heron, D.L., Dietrich, P., Kettler, C., Linol, B., Mottin, T., Vesely, F., Iannuzzi, R., Huyskens, M., Yin, Q.-Z. 2021. High-latitude ice and climate control on sediment supply across SW Gondwana during the Late

Carboniferous and early permian. *Geological Society of America Bulletin*, 133, 2113–2124, doi:10.1130/b35852.1

- Griffis, N., Tabor, N., Stockli, D., Stockli, L., 2023. The Far-Field imprint of the late Paleozoic Ice Age, its demise, and the onset of a dust-house climate across the Eastern Shelf of the Midland Basin, Texas, *Gondwana Research* 115, 17–36, doi:10.1016/j.gr.2022.11.004
- Gulbranson, E. L., Montanez, I. P., Schmitz, M. D., Limarino, C. O., Isbell, J. L., Marensi, S. A., Crowley, J. L. 2010. High-precision U-Pb calibration of Carboniferous glaciation and climate history, Paganzo Group, NW Argentina. *Geological Society of America Bulletin* 122, 1480–1498, doi:10.1130/B30025.1
- Haig, D.W., Dillinger, A., Playford, G., Riera, R., Sadekov, A., Skrzypek, G., Håkansson, E., Mory, A.J., Peyrot, D., Thomas, C. 2022. Methane seeps following early permian (sakmarian) deglaciation, Interior East Gondwana, Western Australia: Multiphase carbonate cements, distinct carbon-isotope signatures, extraordinary biota. *Palaeogeography, Palaeoclimatology, Palaeoecology*, 591, 110862, doi:10.1016/j.palaeo.2022.110862
- Heckel, P.H. 1977. Origin of phosphatic black shale facies in Pennsylvanian cyclothems of Mid-Continent North America. *AAPG Bulletin*, 61, 1045–1068, doi:10.1306/c1ea43c4-16c9-11d7-8645000102c1865d
- Heckel, P.H. 2008. Pennsylvanian cyclothems in Midcontinent North America as far-field effects of waxing and waning of Gondwana Ice Sheets. In: Fielding, C. R., Frank, T. D., Isbell, J. L. (Eds.), *Resolving the Late Paleozoic Ice Age in Time and Space*. Geological Society of America Special Paper, 441, 275–289, doi:10.1130/2008.2441(19)
- Himmler, T., Freiwald, A., Stollhofen, H., Peckmann, J. 2008. Late carboniferous hydrocarbon-seep carbonates from the Glaciomarine Dwyka Group, southern Namibia. *Palaeogeography, Palaeoclimatology, Palaeoecology*, 257, 185–197. doi:10.1016/j.palaeo.2007.09.018
- Holz, M., Souza, P. A., Iannuzzi, R. 2008. Sequence stratigraphy and biostratigraphy of the Late Carboniferous to Early Permian glacial succession (Itararé Subgroup) at the eastern southeastern margin of the Paraná Basin, Brazil. In: Fielding, C. R., Frank, T. D., Isbell, J. L. (Eds.), *Resolving the Late Paleozoic Ice Age in Time and Space*. Geological Society of America Special Paper, 441, 115–129, doi:10.1130/2008.2441(08)
- Holz, M., Franca, A. B., Souza, P. A., Iannuzzi, R., Rohn, R. 2010. A stratigraphic chart of the Late Carboniferous/Permian succession of the eastern border of the Paraná Basin, Brazil, South America. *Journal of South American Earth Sciences*, 29, 381–399, doi:10.1016/j.jsames.2009.04.004
- Hood, W., Cole, R., and Aslan, A. 2009. Anomalous cold in the Pangaeian tropics. *Comment: Geology*, 37, 192, doi:10.1130/G30035C.1

- Isbell, J.L., Miller, M.F., Wolfe, K.L., Lenaker, P.A. 2003. Timing of late Paleozoic glaciation in Gondwana: Was glaciation responsible for the development of northern hemisphere cyclothems? In: Chan, M.A., Archer, A.W. (Eds.), *Extreme depositional environments: Mega end members in geologic time*. Geological Society of America Special Paper, 370, 5–24, doi:10.1130/0-8137-2370-1.5
- Isbell, J.L., Cole, D.I., Catuneanu, O. 2008. Carboniferous-permian glaciation in the main Karoo Basin, South Africa: Stratigraphy, depositional controls, and glacial dynamics. In: Fielding, C. R., Frank, T. D., Isbell, J. L. (Eds.), *Resolving the Late Paleozoic Ice Age in Time and Space*. Geological Society of America Special Paper, 441, 71–82, doi:10.1130/2008.2441(05)
- Isbell, J. L., Henry, L. C., Gulbranson, E. L., Limarino, C. O., Fraiser, M. L., Koch, Z. J., Ciccioli, P. L., Dineen, A. A. 2012. Glacial paradoxes during the late Paleozoic ice age: Evaluating the equilibrium line altitude as a control on glaciation. *Gondwana Research*, 22, 1–19, doi:10.1016/j.gr.2011.11.005
- Koch, J.T., Frank, T.D. 2011. The pennsylvanian–permian transition in the low-latitude carbonate record and the onset of major Gondwanan glaciation. *Palaeogeography, Palaeoclimatology, Palaeoecology*, 308, 362–372, doi:10.1016/j.palaeo.2011.05.041
- Le Heron, D.P., Busfield, M.E., Chen, X., Corkeron, M., Davies, B.J., Dietrich, P., Ghiene, J.-F., Kettler, C., Scharfenberg, L., Vandyk, T.M., Wohlschlägl, R. 2022. New Perspectives on glacial geomorphology in Earth’s Deep time record. *Frontiers in Earth Science*, 10, doi:10.3389/feart.2022.870359
- Le Heron, D.P., Kettler, C., Griffis, N.P., Dietrich, P., Montañez, I.P., Osleger, D.A., Hofmann, A., Douillet, G., Mundil, R. 2021. The late Palaeozoic Ice Age unconformity in southern Namibia viewed as a patchwork mosaic. *The Depositional Record* 8, 419–435, doi:10.1002/dep2.163
- Linol, B., de Wit, M.J., Barton, E., de Wit, M.(M., Guillocheau, F., 2016. U–pb detrital zircon dates and source provenance analysis of Phanerozoic sequences of the Congo Basin, central gondwana. *Gondwana Research*, 29, 208–219, doi:10.1016/j.gr.2014.11.009
- López-Gamundí, O., Limarino, C.O., Isbell, J.L., Pauls, K., Césari, S.N., Alonso-Muruaga, P.J. 2021. The late paleozoic ice age along the southwestern margin of Gondwana: Facies models, age constraints, correlation and sequence stratigraphic framework. *Journal of South American Earth Sciences*, 107, 103056, doi:10.1016/j.jsames.2020.103056
- Macdonald, F.A., Swanson-Hysell, N.L., Park, Y., Lisiecki, L., Jagoutz, O., 2019. Arc-continent collisions in the tropics set Earth’s climate state. *Science*, 364, 181–184, doi:10.1126/science.aav5300
- Marchetti, L., Forte, G., Kustatscher, E., DiMichele, W.A., Lucas, S.G., Roghi, G., Juncal, M.A., Hartkopf-Fröder, C., Krainer, K., Morelli, C., Ronchi, A. 2022. The artinskian warming event: An Euramerican change in climate and the terrestrial Biota during the

early permian. *Earth-Science Reviews*, 226, 103922,  
doi:10.1016/j.earscirev.2022.103922

- Martin, H. 1981. The late Palaeozoic Dwyka Group of the South Kalahari Basin in Namibia and Botswana and the subglacial valleys of the Kaokoveld in Namibia. In: Hambrey, M.J., Harland, W.B. (Eds.), *Earth's Pre-Pleistocene Glacial Record*. Cambridge, UK, Cambridge University Press, 61–66.
- McKenzie, N.R., Horton, B.K., Loomis, S.E., Stockli, D.F., Planavsky, N.J., Lee, C.-T.A. 2016. Continental arc volcanism as the principal driver of icehouse-greenhouse variability. *Science*, 352, 444–447, doi:10.1126/science.aad5787
- Michel, L.A., Tabor, N.J., Montañez, I.P., Schmitz, M.D., Davydov, V.I. 2015. Chronostratigraphy and paleoclimatology of the Lodève Basin, France: Evidence for a pan-tropical aridification event across the carboniferous–permian boundary. *Palaeogeography, Palaeoclimatology, Palaeoecology*, 430, 118–131, doi:10.1016/j.palaeo.2015.03.020
- Milani, E.J., De Wit, M.J. 2008. Correlations between the classic Paraná and Cape–Karoo sequences of South America and Southern Africa and their basin infills flanking the gondwanides: Du Toit revisited. *Geological Society, London, Special Publications*, 294, 319–342, doi:10.1144/sp294.17
- Montañez, I.P., Poulsen, C.J. 2013. The late Paleozoic ice age: An evolving paradigm. *Annual Review of Earth and Planetary Sciences* 41, 629–656, doi:10.1146/annurev.earth.031208.100118
- Montañez, I.P., McElwain, J.C., Poulsen, C.J., White, J.D., DiMichele, W.A., Wilson, J.P., Griggs, G., Hren, M.T. 2016. Climate, pCO<sub>2</sub> and terrestrial carbon cycle linkages during late Palaeozoic glacial-interglacial cycles. *Nature Geoscience* 9, 824–828, doi:10.1038/ngeo2822
- Montañez, I.P. 2021. Current synthesis of the penultimate Icehouse and its imprint on the Upper Devonian through Permian stratigraphic record. *Geological Society, London, Special Publications*, 512, 213–245, doi:10.1144/sp512-2021-124
- Mottin, T.E., Vesely, F.F., Rodrigues, M.C.N.L., Kipper, F., Souza, P.A. 2018. The paths and timing of late Paleozoic ice revisited: New stratigraphic and paleo-ice flow interpretations from a glacial succession in the upper Itararé Group (Paraná Basin, Brazil). *Palaeogeography, Palaeoclimatology, Palaeoecology*, 490, 488–504, doi:10.1016/j.palaeo.2017.11.031
- Nelsen, M.P., DiMichele, W.A., Peters, S.E., Boyce, C.K. 2016. Delayed fungal evolution did not cause the Paleozoic peak in coal production. *Proceedings of the National Academy of Sciences*, 113, 2442–2447, doi:10.1073/pnas.1517943113
- Pfeifer, L.S., Soreghan, G.S., Pochat, S., Van Den Driessche, J., 2020. Loess in eastern equatorial Pangea Archives a dusty atmosphere and possible upland glaciation. *Geological Society of America Bulletin*, 133, 379–392, doi:10.1130/b35590.1

- Richey, J.D., Montañez, I.P., Godderis, Y., Looy, C.V., Griffis, N.P. and DiMichele, W.A. 2020. Influence of temporally varying weatherability on CO<sub>2</sub>–climate coupling and ecosystem change in the late Paleozoic. *Climates of the Past*, 16, 1759–2020, doi:10.5194/cp-16-1759-2020
- Rocha-Campos, A.C., dos Santos, P.R., Canuto, J.R., 2008. Late Paleozoic glacial deposits of Brazil: Paraná basin. In: Fielding, C. R., Frank, T. D., Isbell, J. L. (Eds.), *Resolving the Late Paleozoic Ice Age in Time and Space*. Geological Society of America Special Paper, 441, 97–114, doi:10.1130/2008.2441(07)
- Rønnevik, C., Ksienzyk, A.K., Fossen, H., Jacobs, J., 2017. Thermal evolution and exhumation history of the Uncompahgre Plateau (northeastern Colorado Plateau), based on apatite fission track and (U–th)–he thermochronology and zircon U–Pb dating. *Geosphere*, 13, 518–537, doi:10.1130/ges01415.1
- Rosa, E.L., Vesely, F.F., França, A.B., 2016. A review on late Paleozoic ice-related erosional landforms in the Paraná Basin: Origin and paleogeographical implications. *Brazilian Journal of Geology*, 46, 147–166, doi:10.1590/2317-4889201620160050
- Rosa, E.L.M., Vesely, F.F., Isbell, J.I., Kipper, F., Fedorchuk, N.D. and Souza, P.A. 2019. Constraining the timing, kinematics and cyclicity of Mississippian– Early Pennsylvanian glaciations in the Paraná Basin, Brazil. *Sedimentary Geology*, 384, 29–49, <https://doi.org/10.1016/j.sedgeo.2019.03.001>
- Soreghan, G.S., Soreghan, M.J., Poulsen, C.J., Young, R.A., Eble, C.F., Sweet, D.E., Davogusto, O.C. 2008. Anomalous cold in the Pangaeon Tropics. *Geology*, 36, 659–662, doi:10.1130/g24822a.1
- Soreghan, G.S., Sweet, D.E., Heavens, N.G. 2014. Upland glaciation in Tropical Pangaea: Geologic evidence and implications for late paleozoic climate modeling. *The Journal of Geology*, 122, 137–163, doi:10.1086/675255
- Soreghan, G.S., Soreghan, M.J. and Heavens, N.G. 2019. Explosive volcanisms as a key driver of the Late Paleozoic Ice Age. *Geology*, 47, 600–604, <https://doi.org/10.1130/G46349.1>
- Stollhofen, H., Werner, M., Stanistreet, I.G., Armstrong, R.A. 2008. Single-zircon U–Pb dating of Carboniferous–Permian tuffs, Namibia, and the intercontinental Deglaciation Cycle Framework. In: Fielding, C. R., Frank, T. D., Isbell, J. L. (Eds.), *Resolving the Late Paleozoic Ice Age in Time and Space*. Geological Society of America Special Paper, 441, 83–96, doi:10.1130/2008.2441(06)
- Tabor, N.J., DiMichele, W.A., Montañez, I.P., Chaney, D.S. 2013. Late Paleozoic continental warming of a cold tropical basin and floristic change in Western Pangea. *International Journal of Coal Geology*, 119, 177–186, doi:10.1016/j.coal.2013.07.009
- Tomazelli, L.J., Soliani Júnior, E. 1997. Sedimentary facies and depositional environments related to Gondwana glaciation in Batovi and Suspiro Regions, Rio Grande do Sul, Brazil. *Journal of South American Earth Sciences*, 10, 295–303, doi:10.1016/S0895-9811(97)00019-9

- Torsvik, T., Smethurst, M., Burke, K., Steinberger, B. 2008. Long term stability in deep mantle structure: Evidence from the ~300 Ma Skagerrak-Centered Large igneous province (the SCLIP). *Earth and Planetary Science Letters*, 267, 444–452, doi:10.1016/j.epsl.2007.12.004
- Valdez Buso, V., Aquino, C.D., Paim, P.S., de Souza, P.A., Mori, A.L., Fallgatter, C., Milana, J.P., Kneller, B. 2019. Late Palaeozoic glacial cycles and subcycles in western Gondwana: Correlation of surface and subsurface data of the Paraná Basin, Brazil. *Palaeogeography, Palaeoclimatology, Palaeoecology*, 531, 108435. doi:10.1016/j.palaeo.2017.09.004
- Vesely, F. F., Trzaskos, B., Kipper, F., Assine, M. L., Souza, P. A. 2015. Sedimentary record of a fluctuating ice margin from the Pennsylvanian of western Gondwana; Paraná Basin, southern Brazil. *Sedimentary Geology*, 326, 45–63, doi:10.1016/j.sedgeo.2015.06.012
- Vesely, F.F., Rodrigues, M.C.N.L., da Rosa, E.L.M., Amato, J.A., Trzaskos, B., Isbell, J.L., Fedorchuk, N.D. 2018. Recurrent emplacement of non-glacial diamictite during the Late Paleozoic Ice Age. *Geology* 46, 615–618, doi:10.1130/g45011.1
- Visser, J.N.J. 1983. An analysis of the permo-carboniferous glaciation in the Marine Kalahari Basin, Southern Africa. *Palaeogeography, Palaeoclimatology, Palaeoecology*, 44, 295–315, doi:10.1016/0031-0182(83)90108-6
- Visser, J. N. J. 1997. Deglaciation sequences in the Permo-Carboniferous Karoo and Kalahari basins of Southern Africa; a tool in the analysis of cyclic glaciomarine basin fills. *Sedimentology*, 44, 507–521
- Werner, M. 2006. The Stratigraphy, Sedimentology, and Age of the Late Palaeozoic Mesosaurus Inland Sea, SW Gondwana—New Implications from Studies on Sediments and Altered Pyroclastic Layers of the Dwyka and Ecca Group (Lower Karoo Supergroup) in Southern Namibia [Ph.D. thesis]: Würzburg, University of Würzburg, 425, <http://www.opus-bayern.de/uni-wuerzburg/volltexte/2007/2175/>.
- Williscroft, K., Grasby, S.E., Beauchamp, B., Little, C.T.S., Dewing, K., Birgel, D., Poulton, T., Hryniewicz, K. 2017. Extensive Early Cretaceous (albian) methane seepage on Ellef Ringnes Island, Canadian high arctic. *Geological Society of America Bulletin*, 129, 788–805, doi:10.1130/b31601.1
- Yang, J., Cawood, P.A., Montañez, I.P., Condon, D.J., Du, Y., Yan, J.-X., Yan, S., Yuan, D. 2020. Enhanced continental weathering and large igneous province induced climate warming at the permo-carboniferous transition. *Earth and Planetary Science Letters*, 534, 116074, doi:10.1016/j.epsl.2020.116074
- Zieger, J., Rothe, J., Hofmann, M., Gärtner, A. and Linnemann, U. 2019. The Permo-Carboniferous Dwyka Group of the Aranos Basin (Namibia) –How detrital zircons help understanding sedimentary recycling during a major glaciation. *Journal of African Earth Sciences*, 158, 103555, <https://doi.org/10.1016/j.jafrearsci.2019.103555>.

ACCEPTED MANUSCRIPT

## Figure Captions

**Fig. 1.** Paleogeographic map of late Paleozoic of southwest Gondwana. Sedimentary basins (brown) overlain on present-day Brazil and Uruguay in southeast South America and Namibia, South Africa, Botswana and Angola in southwest Africa. Black arrows indicate ice flow directions across Namibia and Brazil (Visser et al., 1987; Gesicki et al., 2002; Rosa et al., 2016; Assine et al., 2019). Localities: 1 - Anitápolis (from drill core section), Santa Catarina State, 2 – Candiota (from drill core section), Rio Grande do Sul State, 3 – Tses (from outcrop section), Namibia, Aranos subbasin, 4 – Zwartbas (from outcrop section), Namibia, Karasburg subbasin. PR – Paraná State; SC – Santa Catarina State; RGS – Rio Grande do Sul State.

**Fig. 2.** Stratigraphic framework of the late Carboniferous-early Permian for the Paraná and Kalahari basins modified after Griffis et al., 2019; Griffis et al., 2021. Header number above the stratigraphic section refers to map locations in Fig. 1. SB-2 (Sequence-boundary 2) from Holz et al. (2008) in the Anitápolis section, is defined by the juxtaposition of fluvial sandstones on top of marine rocks (>298 Ma). The Taciba Formation is the uppermost unit of the Itararé Group, though in regions of Santa Catarina and Rio Do Sul states, the upper Itararé is referred to as Rio Do Sul Formation (Holz et al., 2010). Correlations into the Kalahari Basin are built based on U-Pb CA-TIMS ages (red stars). All evidence for grounded ice occurs below SB-2 in the Paraná Basin and below the Ganigobis Shale Member and correlative shales in the Zwartbas region in the Kalahari Basin. Letters refer to stratigraphic location of images in Fig. 3. Reported CA-TIMS ages from Griffis et al., 2018; Griffis et al., 2019; Griffis et al., 2021. \* Denotes approximate locations for Quitéria ash (QUT) and striated surface which are projected into the Candiota section (Griffis et al., 2019). Red Samples: ANT1– Anitápolis 1; HNC – Hulha Negra Candiota; CT1 – Canditoa 1; CT3 – Candiota 3; QUT – Quitéria; GS.1 – Ganigobis 1; ZWFUN.1 – Zwartbas 1; ZWFUN.2 – Zwartbas 2; OG-09 – Owl Gorge-09. Prince Al Fm – Prince Albert Formation.

**Fig. 3.** Photographs of glaciogenic features, black shales and volcanic ash from the latest Carboniferous and early Permian described in this study; A) Striated surface, Cachoeira do Sul, Rio Grande do Sul State, Brazil. 30 cm staff for scale; B) Irregular subglacial Dwyka Group contact with basement along the orange river in the Karasburg subbasin, outside the town of Noordoewer, Namibia. Rand coin for scale; C) Rhythmites of the Rio do Sul Formation with outsized clasts in the Anitápolis core, Santa Catarina State, Brazil; D) Outcrop of Ganigobis Shale Member, person for scale; E) Glacial diamictite contact with black shales near Zwartbas. Note large, outsized clast in foreground; F) Volcanic ash (GS.1) within the Ganigobis Shale Member; G) Tonstein located in the Candiota coal units outside of Hulha Negra Candiota. Hammer notes stratigraphic horizon of HNC1; H) Volcaniclastic unit (ANT1) within the lower part of the Rio Bonito Formation in the Anitápolis core.



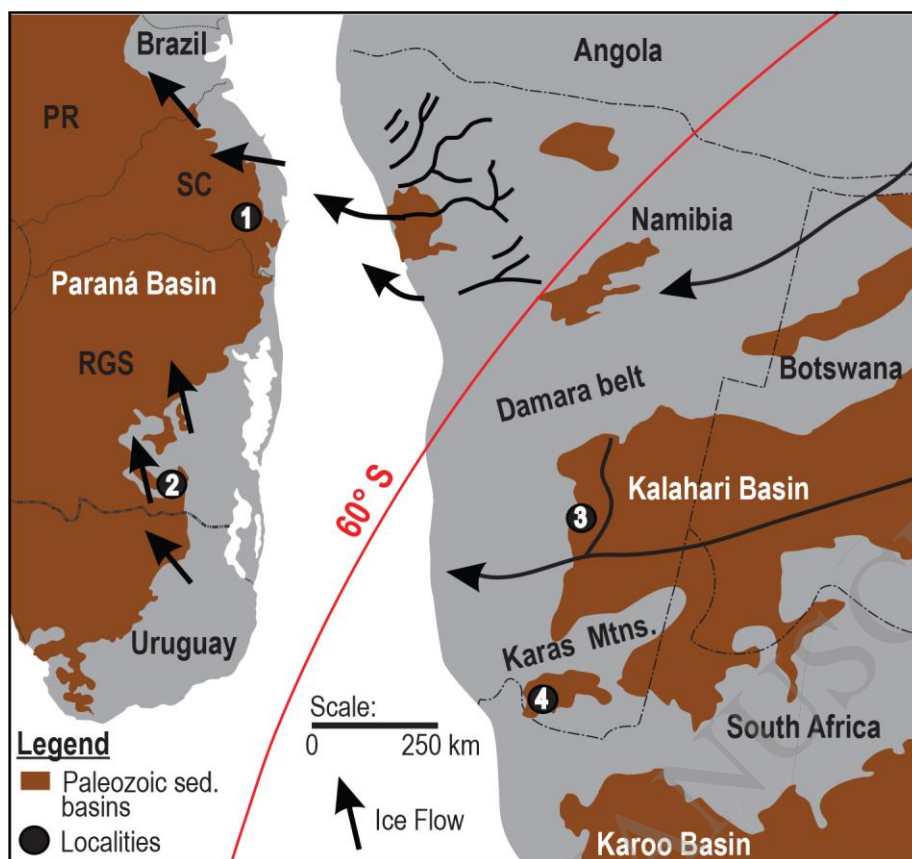


**Figure 1**

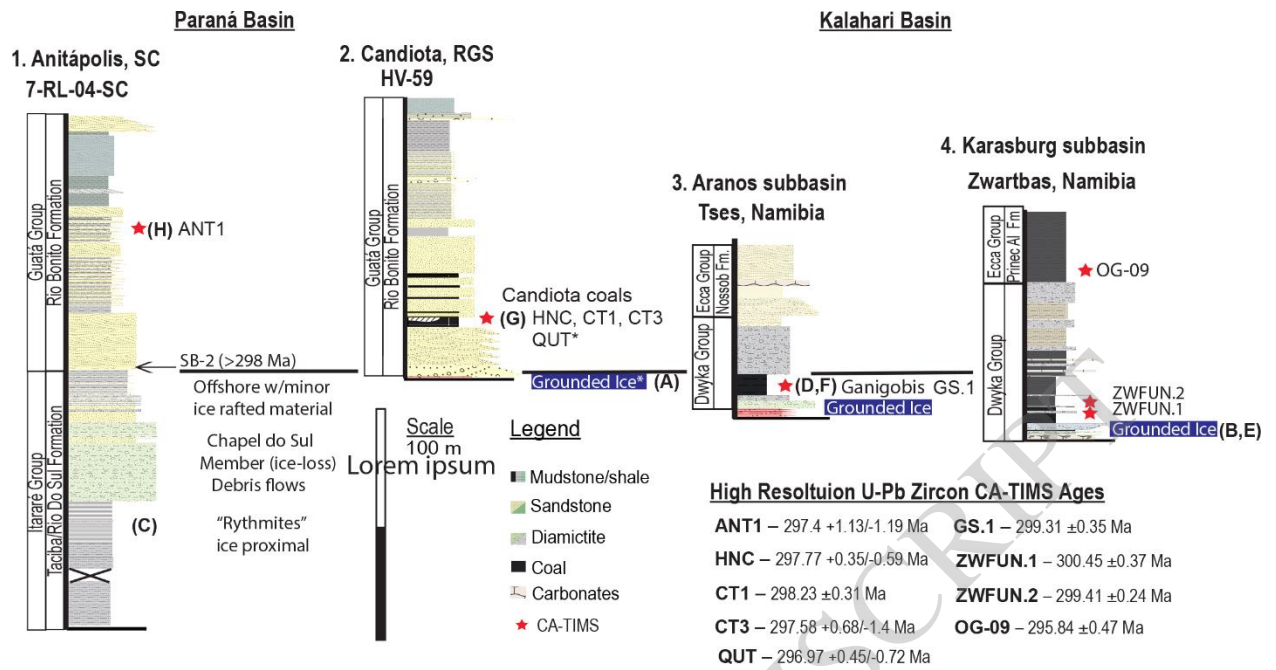


**Figure 2**

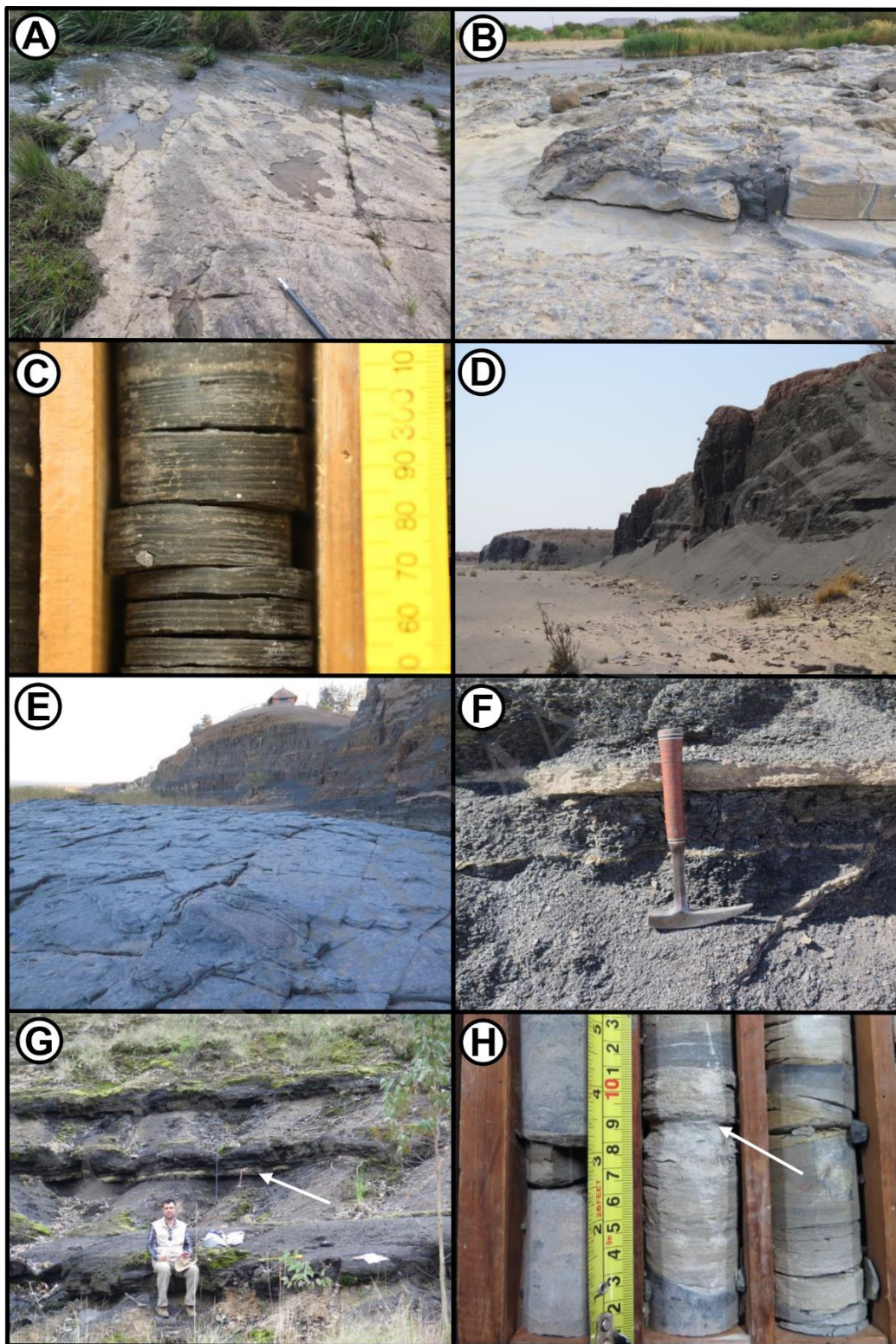


**Figure 3**